SEMARAK ILMU PUBLISHING

Journal of Advanced Research in Applied Sciences and Engineering Technology

https://semarakilmu.com.my/journals/index.php/applied_sciences_eng_tech/index
ISSN: 2462-1943


# Fluid-Structure Interaction Study of The Effect of Stent on Local Hemodynamics Parameters at The Stented Carotid Artery Bifurcation

Nasrul Hadi Johari[1,2,*], M. Hamady[3,4], Xiao Yun Xu[5]

[1] Centre for Advanced Industrial Technology, Universiti Malaysia Pahang, Malaysia
[2] Faculty of Mechanical and Automotive Engineering Technology, Universiti Malaysia Pahang, Malaysia
[3] Department of Interventional Radiology, St Mary's Hospital, Imperial College Healthcare NHS Trust, United Kingdom
[4] Department of Surgery and Cancer, Imperial College London, United Kingdom
[5] Department of Chemical Engineering, Imperial College London, United Kingdom

**ABSTRACT**

Previous fluid-structure interaction (FSI) studies on carotid bifurcation focused on the effect of wall compliance on the predicted hemodynamic features in normal or atherosclerotic carotid arteries. However, FSI study on patient-specific post-stent carotid model is still lacking, and to the authors knowledge no such a study has been reported so far. This study attempts to simulate the full-scale patient-specific post- stent carotid bifurcation geometry with the hope to understand the effect of wall compliance on hemodynamic quantities. The FSI model was based on patient-specific geometry consisting of three components i.e., the carotid artery wall and stent as the solid domain, and blood in the fluid domain. Full FSI simulations incorporating patient-specific boundary conditions at the inlet and outlets, and realistic homogenous incompressible carotid wall and stent were completed to evaluate the flow patterns and wall shear stress. The FSI simulation results were compared with the corresponding rigid-wall model. The quantitative difference in time-averaged wall shear stress (TAWSS) distribution between the FSI and rigid-wall models shows that FSI model predicted 8% less of the area in the low TAWSS band (<0.4%) compared 0.4 - 1.2 Pa. The results suggest that although the effect of wall compliance on flow patterns in the patient-specific post-stent carotid model is negligible, its quantitative effect on wall shear stress may not be trivial and should be considered in future studies.

***Keywords:***
Fluid-structure interaction; carotid artery stenting; restenosis; hemodynamics

**Received: 11 August 2022** **Revised: 17 September 2022** **Accepted: 11 October 2022** **Published: 27 October 2022**

## 1. Introduction

Carotid stenosis is one of the major contributors to the ischemic stroke where blood supply to the brain is cut off. The vulnerable stenosis could rupture, causing thromboembolism where the small pieces of plaque are carried to the small cerebral arterial network and blocking the channels, causing the ischemic stroke. The stenosis can be treated either open surgery called carotid endarterectomy

**Corresponding Author*
*E-mail address: nhadi@ump.edu.my*

https://doi.org/10.37934/ araset.28.2.247255

or by non-invasive procedure called carotid artery stenting (CAS). Although number of CAS patients has increased due to it is less invasive and shorter recovery time, two major concerns related to the efficacy of CAS are the periprocedural risk of vascular events such as death, stroke and myocardial infarction, and long-term risk of restenosis [1–5].

Major clinical trials reported ISR cases after CAS ranging from 5.0 to 17.3% [3–5], which is higher than CEA. Several studies used wall shear stress (WSS) as a hemodynamic risk indicator to identify potential regions of restenosis after CAS [6–9]. Recirculation zones close to the side of the stent struts result in low WSS, which can induce the production of inflammatory molecules, modulate SMC proliferation, and could eventually lead to restenosis.

Previous computational fluid dynamics (CFD) studies of post-stent models have been limited to rigid and fixed geometries for the analysis of flow patterns and WSS. Despite providing a great amount of information on hemodynamic features in carotid models, the rigid wall assumption may have some influence on the predicted flow and WSS distributions [10–13]. FSI simulations have been performed in the studies of human carotid bifurcation [11–13], coronary artery [14], [15] cerebral aneurysm [16], [17], aorta [18], [19], renal artery [20] and aortic aneurysms [21], [22]. The studies by Tang and co-workers [12], [13] on the human carotid bifurcation with atherosclerotic plaque are of particular relevant to the present study, although their models did not include the stent.

This is the first attempt of FSI on the full-scale patient-specific post-stent carotid model with the hope to understand the effect of wall compliance on hemodynamic quantities.

## 2. Methodology

### *2.1 Geometry reconstruction*

The FSI model was reconstructed based on the CTA images of 68-year-old male patient with asymptomatic chronic stenosis (90% according to NASCET grading) in his right internal carotid artery. The patient has undergone carotid artery stenting to remove the presence of a significant fibrocalcific plaque in his carotid. A self-expanding Wallstent (Carotid WALLSTENT$^{TM}$, Boston Scientific, MA, USA) 6-8 x 37 mm was deployed in the ICA and distal to the common carotid artery (CCA). Details patient imaging procedure and geometry reconstruction has been reported in [23]. The post-stent geometry used in this study consists of three components: the carotid wall and stent in the solid domain, and blood in the fluid domain (Figure 1). The complexity in the vicinity of stent struts requires mesh compatibility between the fluid and solid domains during the FSI simulation. To ensure mesh independence, the solid domain was divided into 1.2 million elements, while the fluid domain was discretized into 7 million unstructured tetrahedral elements with local refinement around the stent struts.

### *2.2 Boundary conditions*

The carotid wall was assumed to be a homogenous, incompressible and isotropic elastic material. The wall mechanical properties were described using a linear elastic constitutive model with an elastic modulus of 1 MPa and Poisson's ratio of 0.49, considering the age and medical condition of the patient involved in this study, the carotid wall was assumed to be less compliant with a larger elastic modulus than normal [24]. For the stent, an elastic modulus of 200 GPa and Poisson's ratio of 0.23 were specified.

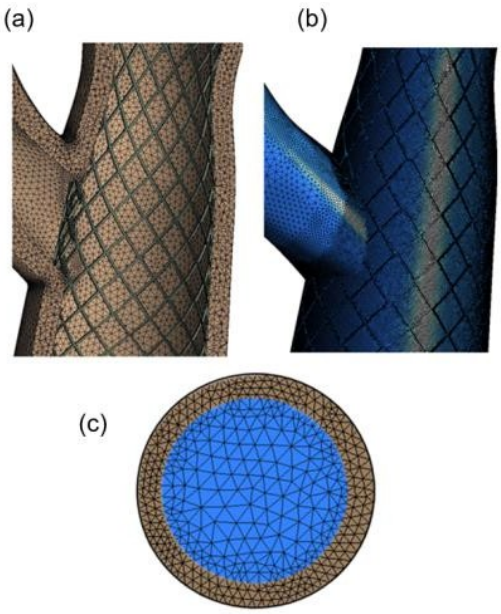


**Fig. 1.** Detailed mesh elements of (a) solid domain (brown) consists of carotid wall and stent, (b) fluid domain (blue) and (c) both domains discretized properly to obtain coincide nodes for fluid-structure interface for FSI simulation.

In the fluid model, the fully developed flow corresponding to Womersley velocity profiles derived from patient-specific common carotid artery (CCA) flow waveforms measured with Doppler ultrasound was assumed at the inlet. At the outlets, pressure waveforms of 3-EWM were prescribed, corresponding to carotid blood pressures of 110 mmHg (systole) and 70 mmHg (diastole) (Figure 2). The no-slip boundary condition was applied to the fluid at the fluid-structure interface. Zero displacement constraints were applied at the CCA inlet and both internal carotid artery (ICA) and external carotid artery (ECA) outlets [14]. For the stent, several nodes at the distal end of the stent were fully constrained along the axial and trans-axial directions.

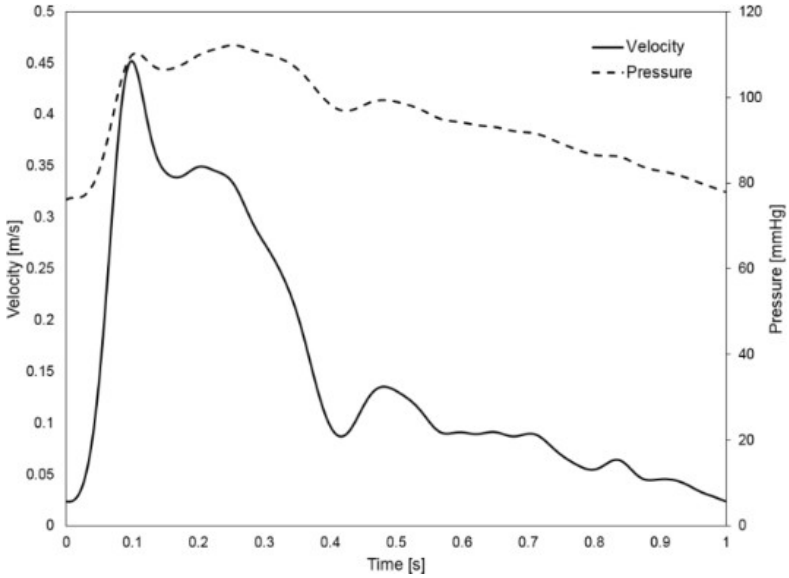


**Fig. 2.** Patient-specific inlet CCA velocity waveform measured by Doppler ultrasound and pressure waveform applied at the outlets of ICA and ECA

### *2.3 FSI simulations*

The arbitrary Lagrangian-Eulerian (ALE) method has been widely used for fully coupled FSI simulations. ALE is preferable for FSI simulations of the cardiovascular system as the fluid-solid interface is properly defined, and the variables are calculated directly at the surfaces. Typically, in a Lagrangian formulation, each node of the mesh element is associated with material properties during motion while in the Eulerian approach, the mesh element is fixed in space and the continuum moves with respect to the grid. Considering a moving reference velocity, the Navier-Stokes equation can be written according to Chiastra *et al*., [14] and Donea *et al*., [25]

$$\rho_F \frac{\partial \mathbf{v}_\mathrm{F}}{\partial t} + \rho_F\big((\mathbf{v}_\mathrm{F} - \mathbf{w}).\nabla \mathbf{v}_\mathrm{F}\big) = -\nabla p + \mu \nabla^2 \mathbf{v}_\mathrm{f} + \mathbf{f}_\mathrm{F}^\mathrm{B} \tag{1}$$

where $\mathbf{v}_\mathrm{F}$ is the velocity vector, $\mathbf{w}$ is the moving mesh velocity vector, $p$ is the pressure, $\mathbf{f}_\mathrm{F}^\mathrm{B}$ is the body force per unit volume, $\rho_F$ is the fluid density. The term $(\mathbf{v}_\mathrm{F} - \mathbf{w})$ directly involved ALE formulation where it represents the relative velocity of the fluid with respect to the moving coordinate velocity.

Meanwhile in the solid domain, the governing equation following the momentum conservation equation can be described as

$$\nabla.\sigma_s + \mathbf{f}_\mathrm{F}^\mathrm{B} = \rho_s \ddot{\mathrm{u}}_\mathrm{s} \tag{2}$$

where $\sigma_s$ is the solid stress tensor, $\rho_s$ is the solid density and $\ddot{\mathrm{u}}_\mathrm{s}$ is the local acceleration of the solid. The fluid and solid domains are then coupled at the FSI interfaces, following two rules: (i) displacements of the fluid and solid domain must be compatible, (ii) tractions at these boundaries must be at equilibrium.

$$\mathrm{u}_\mathrm{s} = \mathrm{u}_\mathrm{F} \tag{3}$$

$$\sigma_s.\mathrm{n}_\mathrm{s} + \sigma_F.\mathrm{n}_\mathrm{F} = 0 \tag{4}$$

Two-way FSI simulation was performed by means of ANSYS Workbench solver using the System Coupling function. The structural model was simulated using ANSYS Mechanical Structural solver and the fluid model using the ANSYS CFX solver. The System Coupling connected both solvers through a series of multi-field time steps, consisting of stagger iterations. The computational time for parallel computing was 6 days for one cardiac cycle using an Intel Xeon E5-2697 workstation with 32 cores and 96GB RAM.

## 3. Results and Discussion

Figure 3 shows instantaneous velocity streamlines obtained with the FSI simulation and the corresponding rigid-wall model. In general, flow patterns at the systolic and deceleration time points were similar, with higher velocities observed at the local 'waist' of the stented region, isolated spots around the stent struts at the opening of ECA, and in the ECA due to its small diameter. Accounting for the wall compliance did not appear to have altered the flow pattern. The stent 'waist-shape' was purposely made in that area due to the presence of extensive fibrocalcific plaque in the arterial wall – to avoid plaque rupture and embolization. This has created a local constriction about 15% from the luminal diameter. Moreover, the position of stent that tilted about 20$^o$ from the host artery has

created local flow disruption at the proximal and distal of the 'waist' area. These geometric features caused local flow disruptions in the proximal region of the constriction especially along the outer wall opposite to the ECA ostium, and at the distal end of the stent. Secondary flow and small recirculation are also observed near the entrance to the stented segment in the CCA where the stent bends about 20° from the host artery. The flow patterns have been recorded by both FSI model and the corresponding rigid-wall model.

Both simulations also indicated a slightly higher TAWSS at the 'waist' of the stented region as a result of local narrowing that caused the jet of the fluid. The effect of wall compliance on flow can be seen clearly in the WSS patterns (Figure 4). Although both models predicted similar locations of high TAWSS at the apex of the bifurcation (> 5 Pa), and low TAWSS in areas proximal and distal to the stent waist, the rigid-wall model displayed a larger area of low TAWSS compared to the FSI model.

For a detailed quantitative comparison, areas with different TAWSS values are expressed as a percentage of the total geometry area, as summarized in Figure 5. The percentage area of low TAWSS (< 0.4 Pa) is 8% larger in the rigid-wall model compared to the FSI model. It is generally accepted that arterial walls experiencing WSS less than 0.4 Pa are at risk of atherosclerosis [26], [27]. Figure 5 clearly shows the similarity in predicted TAWSS patterns between the two models, with the largest wall area experiencing TAWSS in the range of 0.4 - 0.8 Pa, followed by the range of 0.8 - 1.2 Pa. In these two largest TAWSS wall areas, the FSI model was observed with higher percentage than the rigid-wall (71.2% vs 65.2%).

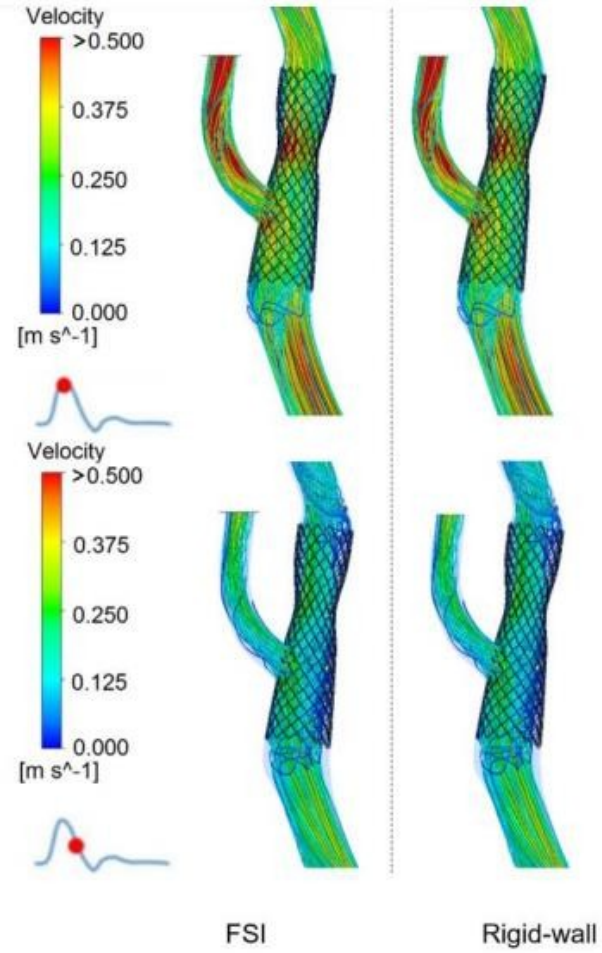


**Fig. 3.** Instantaneous velocity streamlines at peak systole and maximum deceleration in the FSI and rigid-wall post-stent models

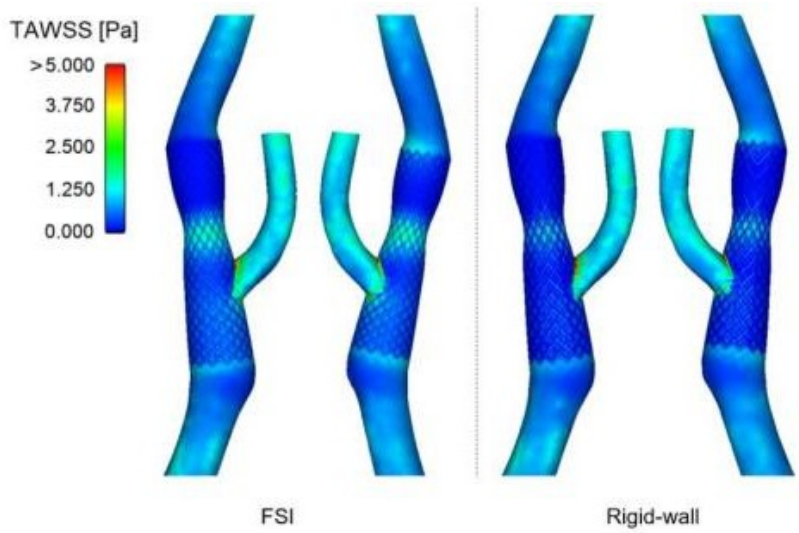


**Fig. 4.** Comparison of TAWSS contours between the FSI and rigid-wall models. Two different views are shown for clarity

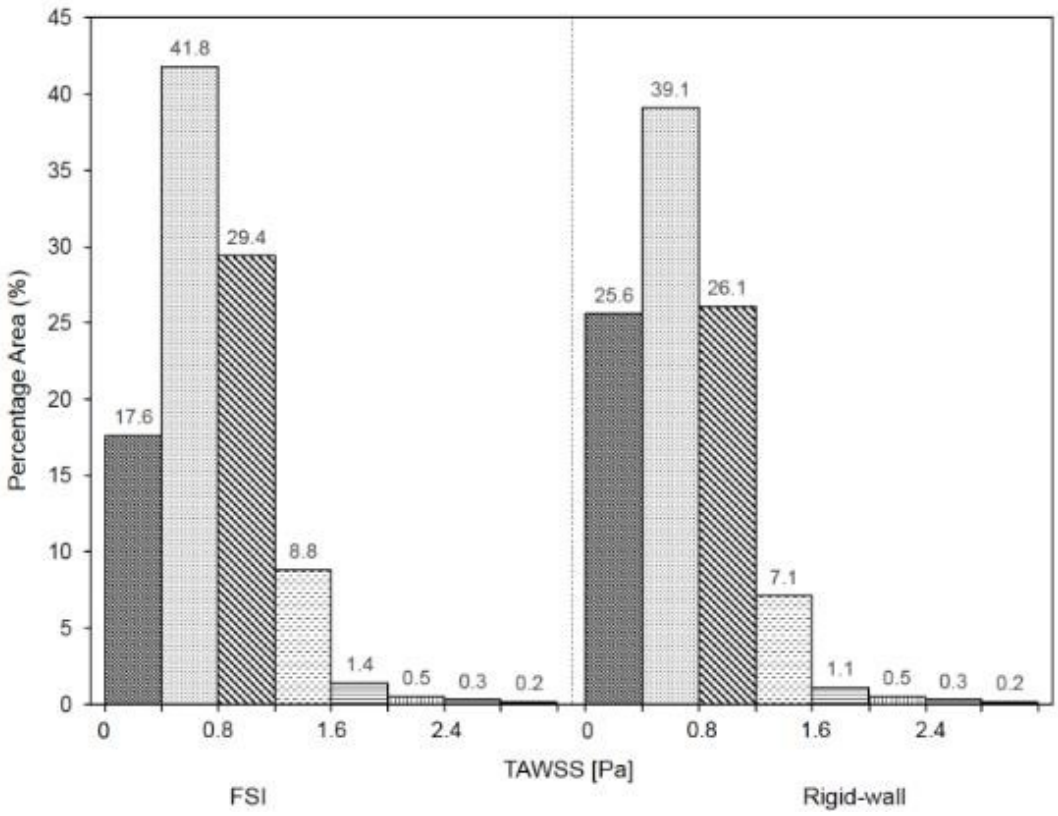


**Fig. 5.** TAWSS distributions percentage area of post-stent model, comparing FSI and rigid-wall models. Each TAWSS bar of the histograms represents the area with a range of 0.4 Pa

The FSI results showed that the rigid-wall model could over-estimate the area of low TAWSS that could lead to the growth of neointimal hyperplasia, causing restenosis. This could be due to the effect of the zero-displacement constraint at the ECA outlet that caused a minimum wall displacement of the bifurcation as well as the stented region. Furthermore, the stiffness of the stent that attached directly to the wall had kept the wall from expand which might reduce the TAWSS in the region. Nevertheless, the results suggest that although the effect of wall compliance on flow patterns in the

patient-specific post- stent carotid model is negligible, its quantitative effect on wall shear stress may not be trivial. The findings on this preliminary work were not applied to the idealized stented arterial models [14], [28]. Studies on idealized stented coronary artery indicated that rigid wall simulations appear adequate for the prediction of near-wall quantities such as WSS.
Nevertheless, future FSI on stented carotid also should include a variable wall thickness and multi-layered wall. A more realistic model for carotid wall material could be implemented in the further studies by considering hyperelastic incompressible isotropic that account multi-layered characteristics of the arterial wall [29]. The tethering of the post-stent model at the inlet and outlets might also affected the accuracy of the simulation result. Moreover, the assumption that was made to reduce the movement of the stent by locally assigned fixed constraints at several points at both ends of the stent could also influenced the TAWSS calculations. Finally, this study also limited only to a single case and should not be generalize for the haemodynamic quantities in relation to the effect of wall compliance in the stented carotid.

## 4. Conclusions

The comparison between FSI and rigid-wall simulations demonstrated that the effect of wall compliance on wall shear stress in the post-stent carotid model is not trivial and should be considered in future studies. The quantitative comparison of TAWSS level showed the rigid-wall simulation predicted slightly larger areas of low TAWSS (< 0.4 Pa) than the FSI, however, the FSI predicted larger areas of TAWSS between 0.4 and 1.2 Pa. Nonetheless, at this point it is worth mentioning even though previous studies using idealized post-stent models reported the effect of wall compliance on coronary artery can be safely ignored [13, 24], results obtained in this study using patient-specific post-stent carotid bifurcation model showed 8% difference in the prediction of TAWSS value lower than 0.4 Pa. Thus, the effect of wall compliance should not be neglected in patient-specific post-stent models.

## Acknowledgement

The authors would like to thank the Ministry of Higher Education for providing financial support under Fundamental Research Grant Scheme (FRGS) No.FRGS/1/2021/TK0/UMP/02/8 (University reference RDU210109) and Universiti Malaysia Pahang for laboratory facilities as well as additional financial support under Internal Research grant RDU190343.

## References

[1] Brott, Thomas G., George Howard, Gary S. Roubin, James F. Meschia, Ariane Mackey, William Brooks, Wesley S. Moore et al. "Long-term results of stenting versus endarterectomy for carotid-artery stenosis." *New England Journal of Medicine* 374, no. 11 (2016): 1021-1031. https://doi.org/10.1056/NEJMoa1505215

[2] Sardar, Partha, Saurav Chatterjee, Herbert D. Aronow, Amartya Kundu, Preethi Ramchand, Debabrata Mukherjee, Ramez Nairooz et al. "Carotid artery stenting versus endarterectomy for stroke prevention: a meta-analysis of clinical trials." *Journal of the American College of Cardiology*69, no. 18 (2017): 2266-2275. https://doi.org/10.1016/j.jacc.2017.02.053

[3] Moon, Karam, Felipe C. Albuquerque, Michael R. Levitt, Azam S. Ahmed, M. Yashar S. Kalani, and Cameron G. McDougall. "The myth of restenosis after carotid angioplasty and stenting." *Journal of neurointerventional surgery* 8, no. 10 (2016): 1006-1010. https://doi.org/10.1136/neurintsurg-2015-011938

[4] Bonati, Leo H., Joanna Dobson, Roland L. Featherstone, Jörg Ederle, H. Bart van der Worp, Gert J. de Borst, P. Th M. Willem et al. "Long-term outcomes after stenting versus endarterectomy for treatment of symptomatic carotid stenosis: the International Carotid Stenting Study (ICSS) randomised trial." *The Lancet* 385, no. 9967 (2015): 529-538. https://doi.org/10.1016/S0140-6736(14)61184-3

[5] Mas, Jean-Louis, Caroline Arquizan, David Calvet, Alain Viguier, Jean-François Albucher, Philippe Piquet, Pierre Garnier et al. "Long-term follow-up study of endarterectomy versus angioplasty in patients with symptomatic

severe carotid stenosis trial." *Stroke* 45, no. 9 (2014): 2750-2756. https://doi.org/10.1161/STROKEAHA.114.005671

[6] Kabinejadian, Foad, Fangsen Cui, Boyang Su, Asawinee Danpinid, Pei Ho, and Hwa Liang Leo. "Effects of a carotid covered stent with a novel membrane design on the blood flow regime and hemodynamic parameters distribution at the carotid artery bifurcation." *Medical & biological engineering & computing* 53, no. 2 (2015): 165-177. https://doi.org/10.1007/s11517-014-1222-2

[7] De Santis, Gianluca, Michele Conti, Bram Trachet, Thomas De Schryver, Matthieu De Beule, Joris Degroote, Jan Vierendeels et al. "Haemodynamic impact of stent–vessel (mal) apposition following carotid artery stenting: mind the gaps!." *Computer methods in biomechanics and biomedical engineering* 16, no. 6 (2013): 648-659. https://doi.org/10.1080/10255842.2011.629997

[8] Uemiya, Nahoko, Chang-Joon Lee, Shoichiro Ishihara, Fumitaka Yamane, Yu Zhang, and Yi Qian. "Analysis of restenosis after carotid artery stenting: preliminary results using computational fluid dynamics based on three-dimensional angiography." *Journal of Clinical Neuroscience*20, no. 11 (2013): 1582-1587. https://doi.org/10.1016/j.jocn.2013.03.042

[9] Filipovic, Nenad, Zhongzhao Teng, Milos Radovic, Igor Saveljic, Dimitris Fotiadis, and Oberdan Parodi. "Computer simulation of three-dimensional plaque formation and progression in the carotid artery." *Medical & biological engineering & computing* 51, no. 6 (2013): 607-616. https://doi.org/10.1007/s11517-012-1031-4

[10] Ningappa, Abhilash Hebbandi, Suraj Patil, Gowrava Shenoy Belur, Augustine Benjamin Valerian Barboza, Nitesh Kumar, Raghuvir Pai Ballambat, Adi Azriff Basri, Shah Mohammed Abdul Khader, and Masaaki Tamagawa. "Influence of Altered Pressures on Flow Dynamics in Carotid Bifurcation System Using Numerical Methods." *Journal of Advanced Research in Fluid Mechanics and Thermal Sciences* 97, no. 1 (2022): 47-61. https://doi.org/10.37934/arfmts.97.1.4761

[11] Lee, Sang Hyuk, Seongwon Kang, Nahmkeon Hur, and Seul-Ki Jeong. "A fluid-structure interaction analysis on hemodynamics in carotid artery based on patient-specific clinical data." *Journal of mechanical science and technology*26, no. 12 (2012): 3821-3831. https://doi.org/10.1007/s12206-012-1008-0

[12] Teng, Zhongzhao, Gador Canton, Chun Yuan, Marina Ferguson, Chun Yang, Xueying Huang, Jie Zheng, Pamela K. Woodard, and Dalin Tang. "3D critical plaque wall stress is a better predictor of carotid plaque rupture sites than flow shear stress: an in vivo MRI-based 3D FSI study." (2010): 031007. https://doi.org/10.1115/1.4001028

[13] Tang, Dalin, Chun Yang, Sayan Mondal, Fei Liu, Gador Canton, Thomas S. Hatsukami, and Chun Yuan. "A negative correlation between human carotid atherosclerotic plaque progression and plaque wall stress: in vivo MRI-based 2D/3D FSI models." *Journal of biomechanics* 41, no. 4 (2008): 727-736. https://doi.org/10.1016/j.jbiomech.2007.11.026

[14] Chiastra, Claudio, Francesco Migliavacca, Miguel Ángel Martínez, and Mauro Malvè. "On the necessity of modelling fluid–structure interaction for stented coronary arteries." *Journal of the mechanical behavior of biomedical materials* 34 (2014): 217-230. https://doi.org/10.1016/j.jmbbm.2014.02.009

[15] Malvè, M., A. García, J. Ohayon, and M. A. Martínez. "Unsteady blood flow and mass transfer of a human left coronary artery bifurcation: FSI vs. CFD." *International communications in heat and mass transfer* 39, no. 6 (2012): 745-751. https://doi.org/10.1016/j.icheatmasstransfer.2012.04.009

[16] Valencia, Alvaro, Patricio Burdiles, Miguel Ignat, Jorge Mura, Eduardo Bravo, Rodrigo Rivera, and Juan Sordo. "Fluid structural analysis of human cerebral aneurysm using their own wall mechanical properties." *Computational and mathematical methods in medicine* 2013 (2013). https://doi.org/10.1155/2013/293128

[17] Takizawa, Kenji, Tyler Brummer, Tayfun E. Tezduyar, and Peng R. Chen. "A comparative study based on patient-specific fluid-structure interaction modeling of cerebral aneurysms." *Journal of Applied Mechanics* 79, no. 1 (2012). https://doi.org/10.1115/1.4005071

[18] Singh, S. D., X. Y. Xu, J. R. Pepper, T. Treasure, and R. H. Mohiaddin. "Biomechanical properties of the Marfan's aortic root and ascending aorta before and after personalised external aortic root support surgery." *Medical Engineering & Physics* 37, no. 8 (2015): 759-766. https://doi.org/10.1016/j.medengphy.2015.05.010

[19] Figueroa, C. Alberto, Irene E. Vignon-Clementel, Kenneth E. Jansen, Thomas JR Hughes, and Charles A. Taylor. "A coupled momentum method for modeling blood flow in three-dimensional deformable arteries." *Computer methods in applied mechanics and engineering* 195, no. 41-43 (2006): 5685-5706. https://doi.org/10.1016/j.cma.2005.11.011

[20] Basri, Adi Azriff, Shah Mohammed Abdul Khader, Cherian Johny, Raghuvir Pai, Muhammad Zuber, Kamarul Arifin Ahmad, and Zanuldin Ahmad. "Numerical Study of Haemodynamics Behaviour in Normal and Single Stenosed Renal Artery using Fluid–Structure Interaction." *Journal of Advanced Research in Fluid Mechanics and Thermal Sciences*51, no. 1 (2018): 91-98.

[21] Lin, Shengmao, Xinwei Han, Yonghua Bi, Siyeong Ju, and Linxia Gu. "Fluid-structure interaction in abdominal aortic

aneurysm: Effect of modeling techniques." *BioMed research international* 2017 (2017). https://doi.org/10.1155/2017/7023078

[22] Tan, F. P. P., R. Torii, A. Borghi, R. H. Mohiaddin, N. B. Wood, and X. Y. Xu. "Fluid-structure interaction analysis of wall stress and flow patterns in a thoracic aortic aneurysm." *International journal of applied mechanics* 1, no. 01 (2009): 179-199. https://doi.org/10.1142/S1758825109000095

[23] Johari, Nasrul Hadi, Mohamad Hamady, and Xiao Yun Xu. "A computational study of the effect of stent design on local hemodynamic factors at the carotid artery bifurcation." *Artery Research* 26, no. 3 (2020): 161-169. https://doi.org/10.2991/artres.k.200603.001

[24] Riley, Ward A., Ralph W. Barnes, Gregory W. Evans, and Gregory L. Burke. "Ultrasonic measurement of the elastic modulus of the common carotid artery. The Atherosclerosis Risk in Communities (ARIC) Study." *Stroke* 23, no. 7 (1992): 952-956. https://doi.org/10.1161/01.STR.23.7.952

[25] Donea, Jean, S. Giuliani, and Jean-Pierre Halleux. "An arbitrary Lagrangian-Eulerian finite element method for transient dynamic fluid-structure interactions." *Computer methods in applied mechanics and engineering* 33, no. 1-3 (1982): 689-723. https://doi.org/10.1016/0045-7825(82)90128-1

[26] Malek, Adel M., Seth L. Alper, and Seigo Izumo. "Hemodynamic shear stress and its role in atherosclerosis." *Jama* 282, no. 21 (1999): 2035-2042. https://doi.org/10.1001/jama.282.21.2035

[27] Razhali, Nur Farahalya, and Ishkrizat Taib. "Analysis of Hemodynamic on Different Stent Strut Configurations in Femoral Popliteal Artery." *CFD Letters* 14, no. 3 (2022): 119-128. https://doi.org/10.37934/cfdl.14.3.119128

[28] Gundert, Timothy J., Alison L. Marsden, Weiguang Yang, and John F. LaDisa Jr. "Optimization of cardiovascular stent design using computational fluid dynamics." (2012): 011002. https://doi.org/10.1115/1.4005542

[29] Sommer, Gerhard, Peter Regitnig, Lukas Költringer, and Gerhard A. Holzapfel. "Biaxial mechanical properties of intact and layer-dissected human carotid arteries at physiological and supraphysiological loadings." *American Journal of Physiology-Heart and Circulatory Physiology* 298, no. 3 (2010): H898-H912. https://doi.org/10.1152/ajpheart.00378.2009